



# A multi-drug resistant HIV-1 protease is resistant to the dimerization inhibitory activity of TLF-PaFf



Ravikiran S. Yedidi<sup>1</sup>, Gheorghe Proteasa, Philip D. Martin, Zhigang Liu<sup>2</sup>, John F. Vickrey, Iulia A. Kovari, Ladislau C. Kovari\*

Queensborough Community College-City University of New York, Bayside, NY 11364, USA

## ARTICLE INFO

### Article history:

Accepted 26 June 2014

Available online 4 July 2014

### Keywords:

HIV/AIDS  
HIV-1 protease  
Dimerization inhibitors  
TLF-PaFf  
X-ray crystallography  
Docking

## ABSTRACT

Human immunodeficiency virus type-1 (HIV-1) protease, a homodimeric aspartyl protease, is a critical drug target in designing anti-retroviral drugs to treat HIV/AIDS. Multidrug-resistant (MDR) clinical isolate-769 HIV-1 protease (PDB ID: 3PJ6) has been shown to exhibit expanded active site cavity with wide-open conformation of flaps (Gly48–Gly52) due to the accumulation of multiple mutations. In this study, an HIV-1 protease dimerization inhibitor (PDI)–TLF–PaFf, was evaluated against MDR769 HIV-1 protease using X-ray crystallography. It was hypothesized that co-crystallization of MDR769 HIV-1 protease in complex with TLF–PaFf would yield either a monomeric or a disrupted dimeric structure. However, crystal structure of MDR769 I10V HIV-1 protease co-crystallized with TLF–PaFf revealed an undisrupted dimeric protease structure (PDB ID: 4NKK) that is comparable to the crystal structure of its corresponding apo-protease (PDB ID: 3PJ6). In order to understand the binding profile of TLF–PaFf as a PDI, docking analysis was performed using monomeric protease (prepared from the dimeric crystal structure, PDB ID: 4NKK) as docking receptor. Docking analysis revealed that TLF–PaFf binds at the N and C termini (dimerization domain) in a clamp shape for the monomeric wild type receptor but not the MDR769 monomeric receptor. TLF–PaFf preferentially showed higher binding affinity to the expanded active site cavity of MDR769 HIV-1 protease than to the termini. Irrespective of binding location, the binding affinity of TLF–PaFf against wild type receptor (–6.7 kcal/mol) was found to be higher compared to its corresponding binding affinity against MDR receptor (–4.6 kcal/mol) suggesting that the MDR769 HIV-1 protease could be resistant to the PDI-activity of TLF–PaFf, thus supporting the dimeric crystal structure (PDB ID: 4NKK).

© 2014 Elsevier Inc. All rights reserved.

## 1. Introduction

Acquired immunodeficiency syndrome (AIDS) is a combination of various opportunistic pathologies in humans that occur when the host immune system is suppressed by the human immunodeficiency virus type-1 (HIV-1) infection [1]. Anti-retroviral drugs that can significantly lower the viral loads in the patients are used in different combinations as highly active anti-retroviral therapy (HAART) [2]. However, rapid incorporation of mutations into

viral genome under clinical drug selection pressure results in the selection of multidrug-resistant variants of HIV-1 [3]. The viral replication cycle involves various viral and host proteins that have been used as drug targets to design inhibitors to prevent the spread of infection. Among the viral proteins, HIV-1 protease is a critical drug target for inhibitor design [4]. Inhibition of the viral protease blocks the cleavage of viral polyproteins and formation of mature viral proteins [5,6]. In the absence of mature viral proteins, the newly produced virions were shown to be non-infectious [7]. Thus, the spread of infection from cell to cell within the host as well as the disease progression are significantly lowered.

Accumulation of multiple drug resistance mutations in the protease as seen in clinical isolate-769 [8] results in the loss of potency of the protease inhibitors (PI). The multidrug-resistant (MDR)-769 HIV-1 protease consists of amino acid substitutions: L10I, M36V, M46L, I54V, I62V, L63P, A71V, V82A, I84V and L90M. Crystal structures of MDR769 HIV-1 protease variants (PDB IDs: ITW7, 3OQ7, 3OQA, 3OQD and 3PJ6) were shown to exhibit

\* Corresponding author at: Department of Biochemistry and Molecular Biology, School of Medicine, Wayne State University, 540 E. Canfield Avenue, Detroit, MI 48201, USA. Tel.: +1 313 993 1335; fax: +1 313 577 2765.

E-mail address: [kovari@med.wayne.edu](mailto:kovari@med.wayne.edu) (L.C. Kovari).

<sup>1</sup> Present address: Experimental Retrovirology Section, HIV and AIDS Malignancy Branch, National Cancer Institute, National Institutes of Health, Bethesda, MD 20892.

<sup>2</sup> Present address: Division of Internal Medicine, Harbor Hospital, Baltimore, MD 21225.

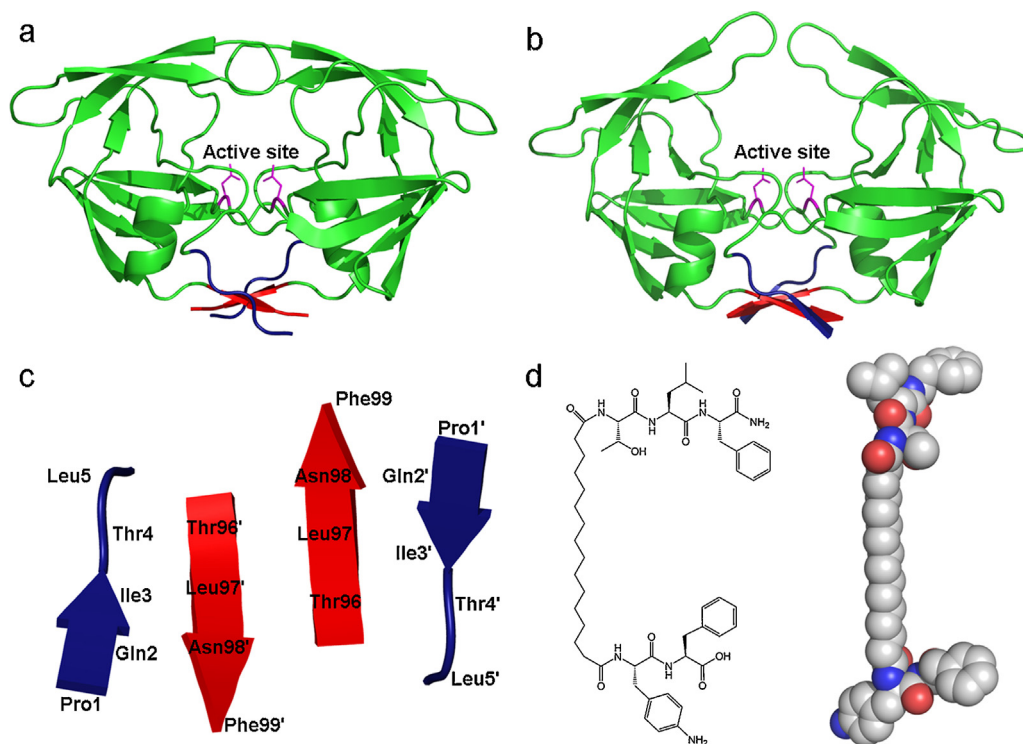


**Fig. 1.** HIV-1 protease dimers, termini interface and the structure of TLF-PaFF. Crystal structures of wild type (taken from PDB ID: 2IEN) and MDR769 I10V (taken from PDB ID: 3PJ6) HIV-1 protease are shown in panels (a) and (b), respectively. In both panels (a) and (b), the protease is shown in green with the catalytic residues highlighted in magenta color stick models. The active site volume of MDR protease is almost two-fold higher than that of the wild type. The N (dark blue) and C (red) termini are highlighted in both panels (a) and (b). An enlarged view focused on the N and C termini is shown in panel (c). The N and C termini of the protease form a strong anti-parallel  $\beta$ -sheet which contributes to the stability of the functional protease dimer. The amino acid residues along the N and C termini are labeled in panel (c), where the numbers were designated as 1–99 for one monomer and 1'–99' for the second monomer. The two-dimensional chemical structure and three-dimensional space filling model of TLF-PaFF are shown in panel d. The TLF moiety is a three amino acid (Thr–Leu–Phe–NH<sub>2</sub>) peptide and the PaFF moiety is a short peptide consisting of *para*-amino phenylalanine and Phe. These two moieties are linked by a hydrocarbon linker. The hydrocarbon linker consists of 16 carbon atoms with two terminal carbonyl groups that are covalently linked to the TLF and PaFF moieties via peptide bonds. (For interpretation of the references to color in this figure legend, the reader is referred to the web version of this article.).

an expanded active site cavity with wide-open conformation of flaps [9,10]. As shown in Fig. 1, the overall volume of the expanded active site cavity in the MDR769 HIV-1 protease is almost two-fold higher compared to that of the wild type. Due to the expanded active site cavity, PIs show loss of contacts [11,12] resulting in loss of potency. Although peptide-inhibitors were recently shown to be active against MDR769 HIV-1 protease [13], bioavailability of such inhibitors could be a concern. Extended lopinavir analogs were recently shown to possess better predicted binding affinities against MDR769 HIV-1 protease [14] and are yet to be evaluated. Hence, there is a constant need for alternative approaches to inhibit the MDR769 HIV-1 protease variants.

In the current study, protease dimerization inhibition approach has been evaluated against the MDR769 HIV-1 protease using X-ray crystallography. Previously, a focused library of protease dimerization inhibitors (PDI) were reported against the wild type HIV-1 protease [15]. No structural data for these PDIs in complex with the protease are available to date. In the current study, one of the PDIs from this library, TLF-PaFF (Fig. 1), was co-crystallized with four clinically relevant variants of MDR769 HIV-1 protease, I10V, A82F, A82S and A82T. The TLF-PaFF consists of two moieties: (a) TLF (Thr–Leu–Phe–NH<sub>2</sub>) and (b) PaFF (*para*-amino Phe–Phe) that are linked through a hydrocarbon chain consisting of 16 carbons. The hydrocarbon chain is coupled on both ends via the terminal carboxyl groups that form peptide bonds with TLF and PaFF moieties. The  $K_i$  values of this class of compounds were reported previously [15]. Normally the N and C termini of the protease form a strong anti-parallel  $\beta$ -sheet (Fig. 1) which contributes to the stability of

the functional protease dimer. The TLF-PaFF was proposed to bind in between the N and C termini of the monomeric protease interfering with the formation of a functional dimer [15]. In the current study, it was hypothesized that the crystal structure of MDR769 HIV-1 protease should either be monomeric or a distorted dimer in the presence of TLF-PaFF. Crystal structure of MDR769 I10V HIV-1 protease co-crystallized with TLF-PaFF was solved and analyzed. Docking studies of TLF-PaFF against wild type HIV-1 protease were performed using AutoDock – Vina [16]. Structural analysis of the crystal structure and docking models was performed to understand the binding of TLF-PaFF.

## 2. Materials and methods

### 2.1. Expression and purification of MDR769 HIV-1 protease variants

Expression and purification of MDR769 HIV-1 protease variants (I10V, A82F, A82S and A82T) were performed as described previously [17]. Briefly, BL21-DE3 (pLysE) *E. coli* cells were used for protease expression. Cultures were induced with 1 mM IPTG and were grown for 4 h. Cells were harvested by centrifugation. Resuspended cells were lysed using a French press to extract the inclusion bodies, which were then dissolved in 6 M urea. Followed by the purification of denatured protease using ion-exchange chromatography, dialysis was performed to refold the protease. Refolded protease was further concentrated using Amicon filters with a molecular weight cut-off of 3 kDa.

## 2.2. Crystallization of MDR769 HIV-1 protease variants

Each protease variant was mixed with 20-fold molar excess of TLF-PaFF (TLF-PaFF was a generous gift from Dr. Jean A. Chmielewski, Department of Chemistry, Purdue University, West Lafayette, IN 47907) and the mixture was incubated for 1 h on ice prior to crystallization. Hanging drop vapor diffusion method was used to set up the crystals. An in-house sodium chloride-based grid screen was used to obtain crystals. For each drop, 1  $\mu$ l of the protease–TLF-PaFF complex was mixed with 1  $\mu$ l of the well solution. Usually crystals were obtained within a week.

## 2.3. X-ray diffraction data collection, processing, structure solutions and refinement

X-ray diffraction data were collected at the beam line ID-5B, DuPont-Northwestern-Dow Collaborative Access Team (DND-CAT), Advanced Photon Source, Argonne National Laboratories, IL. Diffraction data were processed using *MOSFLM* [18] and scaled using *SCALA* [19] through *CCP4* [20] interface. Molecular replacement method – *MOLREP* [21] was used to obtain structure solutions. Crystal structure of MDR769 I10V HIV-1 protease (PDB ID: 3PJ6) was used as search model. Structure solutions were further refined using *REFMAC5* [22]. Electron density maps were generated using *XtalView* [23] program. An initial molecular model of TLF-PaFF was generated by transforming a two-dimensional structure in *ChemDraw Ultra* 10.0 (<http://www.cambridgesoft.com>) to a three-dimensional structure using *Chem3D Pro* 10.0 (<http://www.cambridgesoft.com>) followed by energy minimization to avoid any steric clashes. Refinement libraries for TLF-PaFF were generated using *REFMAC5*. The  $|F_o| - |F_c|$  map was generated and analyzed at contours 2.0–2.5 $\sigma$ . Solvent molecules were built using the solvent building module of *ARP/wARP* [24]. Ramachandran plots were created using *PROCHECK* [25]. Details of diffraction data processing and refinement statistics are given in Table 1. The final refined coordinates for the crystal structure of MDR769 I10V HIV-1 protease co-crystallized with TLF-PaFF were deposited in the Research Collaboratory for Structural Bioinformatics (RCSB) Protein Data Bank (PDB) with accession code: 4NKK.

## 2.4. Docking analysis of TLF-PaFF

All the docking experiments were performed using AutoDock Vina [16] as described previously [10,12,14]. Briefly, PDB IDs: 4NKK (MDR769 HIV-1 protease) and 2IEN (wild type HIV-1 protease) were used as receptors, which were prepared before docking, using AutoDock tools [26] (ADT)-GUI (Graphic User Interface). Ligand, TLF-PaFF was prepared in a similar fashion using ADT-GUI. In each case, the binding pose with highest binding affinity (docking score) was chosen for further structural analysis. All the molecular graphics in this article were prepared using the open source PyMOL (Ver. 0.99rc6) program ([www.pymol.org](http://www.pymol.org)).

## 3. Results

### 3.1. Crystal structure of MDR769 I10V HIV-1 protease co-crystallized with TLF-PaFF revealed a dimeric protease

Among the four MDR769 HIV-1 protease variants (I10V, A82F, A82S and A82T) that were co-crystallized with TLF-PaFF, diffraction quality crystals were obtained for the I10V and A82S variants. While the I10V variant yielded good quality X-ray diffraction data, the A82S diffracted poorly and the data were unusable. Crystal structure of MDR769 I10V HIV-1 protease co-crystallized with TLF-PaFF was solved to 1.8 Å resolution. Data were processed in the space

**Table 1**

X-ray diffraction data and refinement statistics.

Parameters	MDR769 I10V
PDB entry	4NKK
Crystal parameters:	
Resolution range (Å)	35.11–1.56
Unit cell (Å)	$a = b = 44.87$ , $c = 105.36$ , $\alpha = \beta = \gamma = 90^\circ$
Space group	$P4_12_12$
Solvent content (%)	47.0
Data processing:	
No. of unique reflections	16,102 (2,234)
$I/\sigma(I)$	24.3 (3.3)
$R_{\text{merge}}$ (%)	6.6 (50.7)
Data redundancy	13.0 (7.6)
Completeness (%)	99.6 (97.5)
Refinement statistics	
Resolution range (Å)	26.34–1.8
No. of reflections used	10,575
$R_{\text{cryst}}$ (%)	0.204
$R_{\text{free}}$ (%)	0.249
No. of protein atoms	753
No. of water molecules	242
Mean temperature factors ( $\text{\AA}^2$ ):	
Protein	18.59
Main chains	17.22
Side chains	20.10
Waters	27.04
R.M.S.D. bond lengths (Å)	0.007
R.M.S.D. bond angles ( $^\circ$ )	1.113
Ramachandran plot	
Most favored (%)	92.3
Additional allowed (%)	7.7
Generously allowed (%)	0.0
Disallowed (%)	0.0

Values in parentheses are for the highest resolution shell.

$R_{\text{merge}} = \sum |I - \langle I \rangle| / \sum I$ .

$R_{\text{cryst}} = \sum ||F_{\text{obs}}| - |F_{\text{calc}}|| / \sum |F_{\text{obs}}|$ .

group  $P4_12_12$  and structure was solved with one protease monomer per asymmetric unit. Due to weaker intensities at higher resolution, the final structure was refined to 1.8 Å resolution. The  $2|F_o| - |F_c|$  electron density map (Fig. 2) contoured at 2.0 $\sigma$  was analyzed and the refined structure solution of the protease was found to be a dimeric form of the protease. As shown in Fig. 2a, the electron density for protease side chains was clearly visible for both monomers as it would appear for a dimeric form of the protease. No obvious difference electron density was seen for TLF-PaFF around the termini, although very weak and broken density was seen at 2.0–2.5 $\sigma$  in and around the expanded active site cavity. The temperature factors for the TLF-PaFF fit into the broken density were extremely high even after multiple cycles of structure refinement. Although the broken density in the expanded active site cavity indicates weak binding of TLF-PaFF to the dimeric protease as a PI, the focus of the current study is to evaluate TLF-PaFF as a PDI rather than as a PI. Hence, the coordinates for TLF-PaFF were not included in the final structure (PDB ID: 4NKK) due to the above mentioned reasons.

### 3.2. Crystal structure of MDR769 I10V HIV-1 protease co-crystallized with TLF-PaFF did not show the proline-switch mechanism

Crystal structure of the MDR769 I10V HIV-1 apo-protease (PDB ID: 3PJ6) has been previously shown to exhibit a novel Proline-switch (alternate conformations of Pro81 with a  $C_\alpha$  separation of >3 Å) as drug-resistance mechanism [10]. In order to understand the conformational changes in the current structure (PDB ID: 4NKK), it was superposed on to the crystal structure of MDR769 I10V HIV-1 apo-protease (PDB ID: 3PJ6). As shown in Fig. 3a, the  $C_\alpha$  root mean square deviation (RMSD) of the superposed



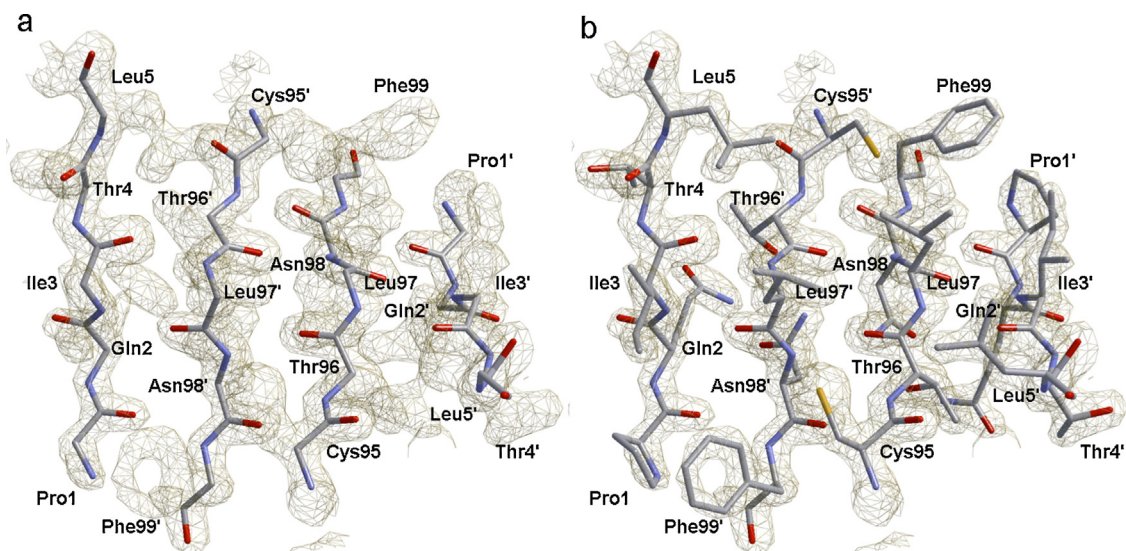


**Fig. 2.** Electron density map of the termini. The  $2|F_o| - |F_c|$  map contoured at  $2.0\sigma$  covering the N and C termini of the MDR769 I10V HIV-1 protease (PDB ID: 4NKK) is shown in olive green color. Panel (a) shows only the main chain of the protease (stick model with gray carbon atoms, blue nitrogen atoms and red oxygen atoms) for clarity while panel (b) shows both main chain and the side chains (stick model with gray carbon atoms, blue nitrogen atoms and red oxygen atoms). The electron density is shown for both main chain as well as side chains in both panels. The two monomers of the protease are distinguished by the amino acid labeling. Residues from monomer-1 are labeled as Pro1–Leu5/Cys95–Phe99 while the residues from monomer-2 are labeled as Pro1'–Leu5'/Cys95'–Phe99'. The electron density clearly indicates a dimeric form of the protease in the presence of TLF–PafF. No density for TLF–PafF was seen around the termini. (For interpretation of the references to color in this figure legend, the reader is referred to the web version of this article.).

structures indicates no significant structural deviations around the termini. RMSD values  $<1.0 \text{ \AA}$  were considered biologically insignificant. Pro81, an active site residue that is critical in ligand binding, showed a significantly high RMSD of  $3.0 \text{ \AA}$  in the current structure (PDB ID: 4NKK) when compared to its corresponding apo-protease structure (PDB ID: 3PJ6). The side chain of Pro81 in the current structure (PDB ID: 4NKK) showed only one conformation (absence of Proline-switch) pointing towards the expanded active site cavity comparable to that of the wild type protease. Glu35, a non-active site, surface residue that may not play a critical role in ligand binding, showed a minor RMSD of  $<1.5 \text{ \AA}$ . Analysis of the superposed structures revealed that the 80s loop was stabilized (Fig. 3b) in the current structure (PDB ID: 4NKK) indicating that TLF–PafF may bind

in or around the expanded active site cavity of the dimeric protease, but with very weak affinity due to lack of contiguous electron density. These results indicate that TLF–PafF, in spite of stabilizing the 80s loop, failed to block the formation of the dimeric protease, suggesting that the MDR769 I10V HIV-1 protease could be resistant to the PDI activity of TLF–PafF.

### 3.3. TLF–PafF binds in the expanded active site cavity of the monomeric MDR769 I10V HIV-1 protease docking receptor

In the absence of convincing electron density for TLF–PafF in the crystal structure, the dimeric MDR769 I10V HIV-1 protease structure (PDB ID: 4NKK) was used as a docking receptor and the docking

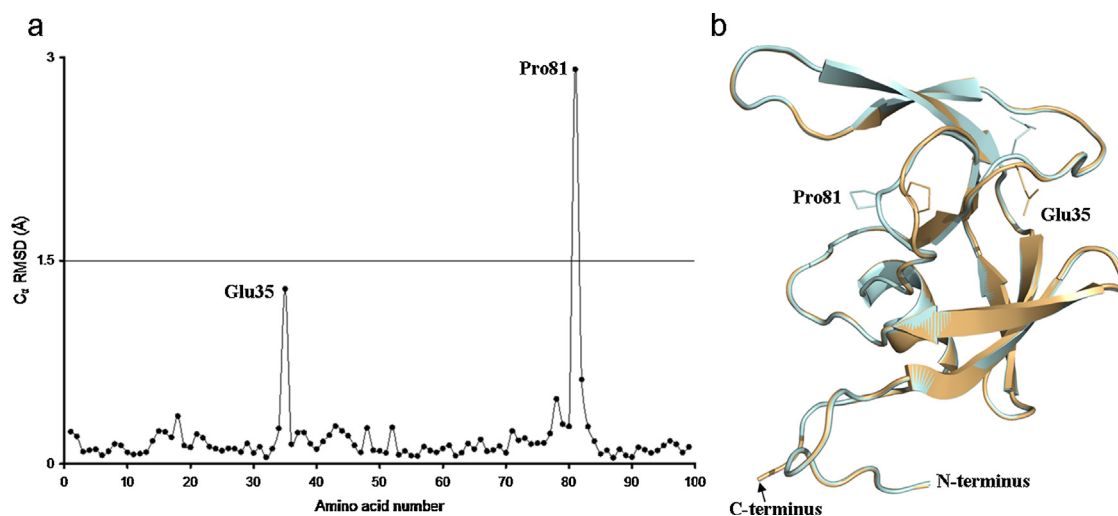


**Fig. 3.** Superposition of apo and complex proteases. Root mean square deviation (RMSD) of  $C_\alpha$  atoms of the MDR769 I10V HIV-1 protease from PDB ID: 4NKK superposed onto the corresponding  $C_\alpha$  atoms of the apo-protease (taken from PDB ID: 3PJ6) is shown in panel (a). RMSD values  $<1.0 \text{ \AA}$  were considered biologically insignificant. Glu35 and Pro81 showed significant RMSD values among the 99 amino acid residues. Panel (b) shows the corresponding superposed protease structures from PDB ID: 3PJ6 (shown in gold color) and PDB ID: 4NKK (shown in silver blue color). Side chains of residues Glu35 and Pro81 are shown as stick models and are labeled accordingly. The structure from 4NKK shows stabilized 80s loop with normal conformation of Pro81 (comparable to that of the wild type protease) while the apo structure shows Proline-switch mechanism reported earlier [10]. Pro81 is one of the critical ligand binding residues in the active site while Glu35 is a non-active site, surface residue that may not play direct role in inhibitor binding. (For interpretation of the references to color in this figure legend, the reader is referred to the web version of this article.).

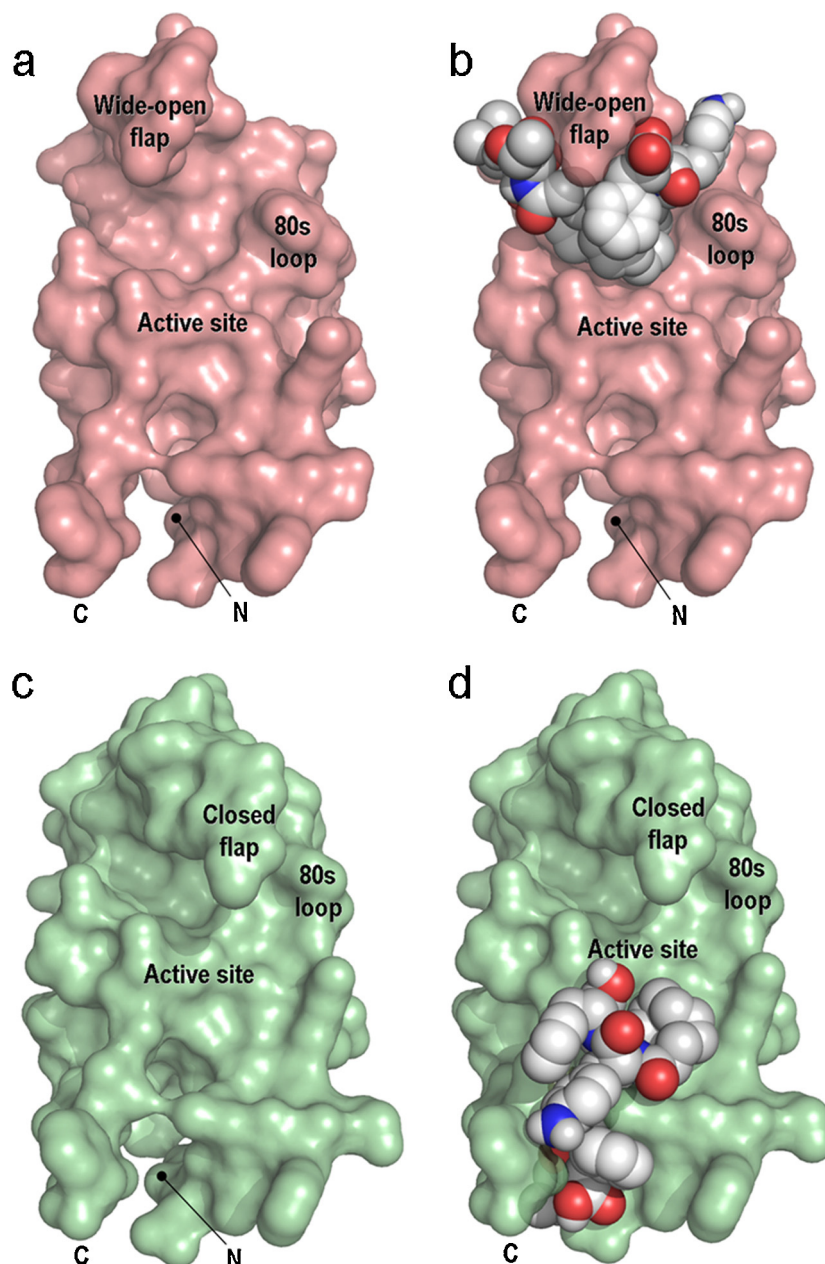


**Fig. 4.** Monomeric docking receptors and solutions. Panels (a) and (b) show the monomeric MDR769 I10V receptor (prepared from PDB ID: 4NKK) before and after docking with the TLF-PaFF (shown as space filling model with white color carbon atoms), respectively. In both panels (a) and (b), the MDR receptor shows wide-open conformation of the flap with an expanded active site cavity. Panels (c) and (d) show the monomeric wild type receptor (prepared from PDB ID: 2IEN) before and after docking with TLF-PaFF, respectively. In both panels (c) and (d), the wild type receptor shows a closed flap conformation. The binding poses shown here were chosen based on the highest binding affinity (docking score) against the MDR (−4.6 kcal/mol) and wild type (−6.7 kcal/mol) receptors. The TLF-PaFF preferentially binds in the expanded active site cavity of the MDR receptor while it binds at the termini in the case of wild type receptor.

**Table 2**

Polar and hydrophobic contacts made by TLF-PaFF with MDR769 and wild type HIV-1 protease monomeric receptors.

Receptor	<sup>a</sup> B.A. (kcal/mol)	Polar contacts	Hydrophobic contacts	<sup>b</sup> Total
<sup>c</sup> MDR769	−4.6	G48 <sup>d</sup> (2)	A28 (2), D29 (1), V32 (1), I47 (5), G48 (2), I50 (3), F53 (2), V54 (1), P79 (3), P81 (1), V84 (3)	26
<sup>e</sup> WT	−6.7	P1 (1), I3 (1), D25 (1), T26 (1), G27 (1), T96 (4), N98 (2)	Q2 (2), I3 (1), T4 (1), L5 (4), R8 (1), P9 (1), L23 (3), L24 (2), D25 (1), T26 (1), G27 (1), A95 (1), L97 (2), N98 (2), F99 (1)	35

<sup>a</sup>B.A. – binding affinity.

<sup>b</sup>Total is the sum of polar and hydrophobic contacts listed in columns 3 and 4 for each receptor.

<sup>c</sup>MDR769 I10V HIV-1 protease monomeric receptor prepared from PDB ID: 4NKK.

<sup>d</sup>Values in parentheses indicate number of contacts (either polar or hydrophobic) between the receptor and TLF-PaFF.

<sup>e</sup>Wild type HIV-1 protease monomeric receptor prepared from PDB ID: 2IEN.

solution of TLF-PaFF was found to be bound in the expanded active site cavity of the dimeric MDR769 I10V HIV-1 protease as a PI with a binding affinity (docking score) of  $-6.7$  kcal/mol (details not shown here as the focus of this study is to analyze the TLF-PaFF as a PDI rather than as a PI). In order to understand the binding profile of TLF-PaFF as a PDI, further docking analysis was performed by using a monomeric MDR769 I10V HIV-1 protease as receptor. The monomeric receptor, as shown in Fig. 4a, was prepared from the dimeric crystal structure (PDB ID: 4NKK) by removing the coordinates for one of the monomers. Choosing one monomer over the other monomer from the dimeric structure (PDB ID: 4NKK) may not be relevant as the structure was solved in the space group  $P4_12_12$  with one monomer per asymmetric unit and the biological dimer consists of identical monomers. The binding pose of TLF-PaFF shown in Fig. 4b was chosen based on its highest binding affinity (docking score) value of  $-4.6$  kcal/mol. This binding pose was found to be bound in the expanded active site area close to the wide-open flaps and the 80s loops but not at the dimerization interface of the N and C termini. Analysis of contacts revealed that TLF-PaFF is involved in two polar contacts with the backbone carbonyl oxygen atom of Gly48 and 24 hydrophobic contacts. Details of hydrophobic contacts are given in Table 2. Two other binding poses of TLF-PaFF, as shown in Fig. S1, with binding affinity (docking score) of  $-4.5$  kcal/mol each, were also analyzed. None of the three poses were found to be bound at the N and C termini of the MDR769 I10V HIV-1 protease. These docking analyses suggest that the TLF-PaFF has very weak affinity to the termini and preferentially binds in the expanded active site cavity of the monomeric MDR769 I10V HIV-1 protease receptor.

#### 3.4. TLF-PaFF binds to the termini of the monomeric wild type HIV-1 protease docking receptor

TLF-PaFF was docked against a monomeric form of wild type HIV-1 protease receptor, shown in Fig. 4c, prepared from the crystal structure, PDB ID: 2IEN. As shown in Fig. 4d, docking analysis revealed a favorable binding pose with highest binding affinity (docking score) of  $-6.7$  kcal/mol. This binding pose was found to be bound in between the N and C termini of the wild type HIV-1 protease receptor with relatively higher binding affinity ( $-6.7$  kcal/mol) than that of the MDR protease receptor ( $-4.6$  kcal/mol). The TLF moiety of TLF-PaFF was bound in between the N and C termini as proposed previously [15] and the hydrocarbon chain of TLF-PaFF extended into the active site cavity as an inverted clamp with the PaFF moiety pointing towards the C-terminus of the protease. Eleven polar contacts (Table 2) were seen between TLF-PaFF and wild type protease of which, eight were found to be with residues from the N and C termini while three were seen, one each, with the catalytic triad (Asp25, Thr26 and Gly27) in the active site area often referred to as the “fireman’s grip” [27]. As shown in Table 2, out of 24 hydrophobic contacts made by TLF-PaFF with wild type protease, 13 were found to be with residues from N and C termini. An additional binding pose of TLF-PaFF that yielded a lower binding affinity ( $-5.6$  kcal/mol) (Fig. S1), was also analyzed but this pose was found to be bound in the active site area in a similar fashion to that of the MDR protease. These results suggest that the TLF-PaFF shows higher binding affinity to the N and C termini ( $-6.7$  kcal/mol) than to the active site area ( $-5.6$  kcal/mol) of the monomeric wild type HIV-1 protease receptor.

## 4. Discussion

In the current study, crystal structure of MDR769 I10V HIV-1 protease co-crystallized with TLF-PaFF (PDB ID: 4NKK) showed a dimeric form of the protease suggesting that the MDR769 I10V

HIV-1 protease is resistant to the PDI activity of TLF-PaFF. It was hypothesized that in the presence of TLF-PaFF, the overall structure of the MDR769 I10V HIV-1 protease should either be monomeric or a distorted dimer. Our results showed that the crystal structure of MDR769 I10V HIV-1 protease in the presence of TLF-PaFF was dimeric and almost identical to its corresponding apo-protease structure (PDB ID: 3PJ6). Previously, it has been shown that the I10V variant of MDR769 exhibits an unusual “Proline Switch” (PDB ID: 3PJ6) in the 80s loop (Pro79–Val84) as a drug resistance mechanism [10]. In the current structure (PDB ID: 4NKK), no such proline switch mechanism was seen in the presence of TLF-PaFF suggesting that the TLF-PaFF might still bind in the expanded active site cavity of the dimeric protease as a PI but with a very weak affinity due to lack of convincing electron density.

The dimeric structure of the MDR protease can be reasoned mainly in two ways: (a) MDR769 I10V HIV-1 protease is resistant to the PDI activity of TLF-PaFF and (b) TLF-PaFF is unable to dissociate the pre-formed MDR protease dimers. Crystal structures of MDR769 HIV-1 protease variants (PDB IDs: 1TW7, 3OQ7, 3OQA, 3OQD and 3PJ6) have been shown to exhibit a conserved wide-open conformation of the flaps with expanded active site cavity. Due to the availability of additional chemical space in the expanded active site cavity, docking analysis using the monomeric MDR receptor prepared from the dimer structure (PDB ID: 4NKK) showed that TLF-PaFF has almost similar binding affinity within the active site area of the MDR769 I10V HIV-1 protease irrespective of its binding location (Fig. 4b and Fig. S1). In the case of wild type protease, due to the availability of relatively lesser chemical space in the active site area, the TLF-PaFF has higher binding affinity to the termini ( $-6.7$  kcal/mol) (Fig. 4d) rather than the active site area ( $-5.6$  kcal/mol) (Fig. S1) with  $>1.0$  kcal/mol. difference in its binding affinity. Irrespective of the binding site, TLF-PaFF showed higher binding affinity to the monomeric wild type protease receptor than to the monomeric MDR protease receptor. Thus, the current dimeric crystal structure (PDB ID: 4NKK) with wide-open flaps and the docking analysis suggest that the MDR769 I10V HIV-1 protease could be resistant to the PDI activity of TLF-PaFF. In the current study, MDR769 I10V HIV-1 protease was purified and refolded from the *E. coli* inclusion bodies in the absence of TLF-PaFF. In such case, one can predict the majority of protease molecules to be mature dimers with pre-occupied N and C termini (due to the formation of dimers). One can hypothesize that the wild type protease exists in a dynamic equilibrium of monomeric and dimeric forms where TLF-PaFF can potentially inhibit the formation of dimers but our current structural analyses show that TLF-PaFF failed to inhibit the formation of dimeric protease in the case of MDR769 I10V HIV-1 protease. This suggests that majority of MDR769 I10V HIV-1 protease molecules exist as mature stable dimers (as seen in the crystal structure, PDB ID: 4NKK) with a minor population of monomeric form and the monomeric form is resistant to TLF-PaFF due to weak binding affinity of TLF-PaFF to the N and C termini of the monomeric MDR769 I10V HIV-1 protease receptor.

Biochemically, the flap conformation of HIV-1 protease is flexible in a solution depending on the presence or absence of various ligands. Typically, wild type HIV-1 protease has been shown to exhibit either closed (in the presence of ligand, PDB ID: 2IEN) or open (apo-form, PDB ID: 2PC0) conformations of the flap while the MDR769 variants have been shown to exhibit mostly a wide-open conformation of the flaps either in the presence (PDB IDs: 1RV7, 3R0W, 3R0Y, 4EYR, 4L1A) or absence (PDB IDs: 1TW7, 3PJ6, 3OQ7, 3OQA, 3OQD) of ligand. The monomeric docking receptors for MDR769 I10V (Fig. 4a) and wild type (Fig. 4c) HIV-1 protease variants that were used in this study contain wide-open and closed conformation of the flaps, respectively. One can reason that the difference in binding poses of TLF-PaFF docked against either receptor (Fig. 4b and d) could be due to the receptor-flap conformation.



Irrespective of the protease flap conformation, TLF-PaFf has been biochemically shown to inhibit the wild type HIV-1 protease as a PDI with a reasonable  $K_i$  value [15]. Additionally, one can also reason that using an MDR receptor with closed conformation of the flaps may change the binding pose of TLF-PaFf. However, the current co-crystal structure (PDB ID: 4NKK) clearly demonstrated the wide-open conformation of the MDR protease flaps as well as the dimeric form of the MDR protease in the presence of TLF-PaFf suggesting that the closed flap conformation of the MDR receptor may not be relevant. Taken together, based on the current docking analysis, TLF-PaFf failed to bind the termini of the monomeric MDR769 I10V HIV-1 protease receptor with wide-open flaps supporting the dimeric crystal structure (PDB ID: 4NKK).

In summary, crystal structure of MDR769 I10V HIV-1 protease co-crystallized with a PDI (TLF-PaFf) showed a dimeric form of the protease suggesting that the MDR769 I10V HIV-1 protease could be resistant to the PDI activity of TLF-PaFf. The PDI, TLF-PaFf preferentially binds in the expanded active site area of the monomeric MDR769 I10V HIV-1 protease receptor rather than to the termini. TLF-PaFf binds in an inverted clamp shape near the termini of monomeric wild type protease receptor with relatively higher binding affinity. Based on our current structural analyses, it can be concluded that the expanded active site cavity with wide-open flaps and proline switch mechanism of MDR769 I10V HIV-1 protease variant influence the binding affinity of TLF-PaFf thus causing PDI-resistance. It may be worthwhile to further investigate whether TLF-PaFf can inhibit the formation of dimers by refolding the denatured MDR769 HIV-1 protease variants in the presence of TLF-PaFf. However, this extended study is beyond the scope of this article

## Acknowledgements

We thank Dr. Jean Chmielewski for providing us TLF-PaFf. We thank the National Institutes of Health for funding to LCK (grant # AI65294). Portions of this work were performed at the DuPont-Northwestern-Dow Collaborative Access Team (DND-CAT) located at Sector 5 of the Advanced Photon Source (APS). DND-CAT is supported by E. I. DuPont de Nemours & Co., The Dow Chemical Company and Northwestern University. Use of the APS, an Office of Science User Facility operated for the US Department of Energy (DOE) Office of Science by Argonne National Laboratory, was supported by the U.S. DOE under Contract No. DE-AC02-06CH11357.

## Appendix A. Supplementary data

Supplementary data associated with this article can be found, in the online version, at <http://dx.doi.org/10.1016/j.jmgm.2014.06.010>.

## References

- [1] R.A. Weiss, How does HIV cause AIDS, *Science* 260 (1993) 1273–1279.
- [2] J. Stephenson, The art of 'HAART': researchers probe the potential and limits of aggressive HIV treatments, *JAMA* 277 (1997) 614–616.
- [3] R.W. Shafer, S.Y. Rhee, D. Pillay, et al., HIV-1 protease and reverse transcriptase mutations for drug resistance surveillance, *AIDS* 21 (2007) 215–223.
- [4] C. Debouck, The HIV-1 protease as a therapeutic target for AIDS, *AIDS Res. Hum. Retroviruses* 8 (1992) 153–164.
- [5] C. Peng, B.K. Ho, T.W. Chang, et al., Role of human immunodeficiency virus type 1-specific protease in core protein maturation and viral infectivity, *J. Virol.* 63 (1989) 2550–2556.
- [6] N.E. Kohl, E.A. Emini, W.A. Schleif, et al., Active human immunodeficiency virus protease is required for viral infectivity, *Proc. Natl. Acad. Sci. U.S.A.* 85 (1998) 4686–4690.
- [7] D.M. Lambert S.R.Jr., C.E. Petteway, McDaniel, et al., Human immunodeficiency virus type 1 protease inhibitors irreversibly block infectivity of purified virions from chronically infected cells, *Antimicrob. Agents Chemother.* 36 (1992) 982–988.
- [8] S. Palmer, R.W. Shafer, T.C. Merigan, Highly drug-resistant HIV-1 clinical isolates are cross-resistant to many antiretroviral compounds in current clinical development, *AIDS* 13 (1999) 661–667.
- [9] P. Martin, J.F. Vickrey, G. Proteasa, et al., Wide-open 1.3 Å structure of a multidrug-resistant HIV-1 protease as a drug target, *Structure* 13 (2005) 1887–1895.
- [10] R.S. Yedidi, G. Proteasa, J.L. Martinez, et al., Contribution of the 80's loop of HIV-1 protease to the multidrug-resistant mechanism: crystallographic study of MDR769 HIV-1 protease variants, *Acta Crystallogr. D: Biol. Crystallogr.* 67 (2011) 524–532.
- [11] R.S. Logsdon, J.F. Vickrey, P. Martin, et al., Crystal structures of a multidrug-resistant human immunodeficiency virus type 1 protease reveal an expanded active-site cavity, *J. Virol.* 78 (2004) 3123–3132.
- [12] R.S. Yedidi, Z. Liu, Y. Wang, et al., Crystal structures of multidrug-resistant HIV-1 protease in complex with two potent anti-malarial compounds, *Biochem. Biophys. Res. Commun.* 421 (2012) 413–417.
- [13] R.S. Yedidi, J.M. Muhuhi, Z. Liu, et al., Design, synthesis and evaluation of a potent substrate analog inhibitor identified by scanning Ala/Phe mutagenesis, mimicking substrate co-evolution, against multidrug-resistant HIV-1 protease, *Biochem. Biophys. Res. Commun.* 438 (2013) 703–708.
- [14] R.S. Yedidi, Z. Liu, I.A. Kovari, et al., P1 and P1' para-fluoro phenyl groups show enhanced binding and favorable predicted pharmacological properties: structure-based virtual screening of extended lopinavir analogs against multidrug resistant HIV-1 protease, *J. Mol. Graph. Model.* 47 (2014) 18–24.
- [15] M.D. Shultz, Y.W. Ham, S.G. Lee, et al., Small-molecule dimerization inhibitors of wild-type and mutant HIV protease: a focused library approach, *J. Am. Chem. Soc.* 126 (2004) 9886–9887.
- [16] O. Trott, A.J. Olson, AutoDock Vina: improving the speed and accuracy of docking with a new scoring function, efficient optimization and multithreading, *J. Comput. Chem.* 31 (2010) 455–461.
- [17] J.F. Vickrey, B.C. Logsdon, G. Proteasa, et al., HIV-1 protease variants from 100-fold drug resistant clinical isolates: expression, purification, and crystallization, *Protein Expr. Purif.* 28 (2003) 165–172.
- [18] A.G. Leslie, The integration of macromolecular diffraction data, *Acta Crystallogr. D: Biol. Crystallogr.* 62 (2006) 48–57.
- [19] P. Evans, Scaling and assessment of data quality, *Acta Crystallogr. D: Biol. Crystallogr.* 62 (2006) 72–82.
- [20] Collaborative Computational Project, Number 4, The CCP4 suite: programs for protein crystallography, *Acta Crystallogr. D: Biol. Crystallogr.* 50 (1994) 760–763.
- [21] A. Vagin, A. Teplyakov, MOLREP: an automated program for molecular replacement, *J. Appl. Crystallogr.* 30 (1997) 1022–1025.
- [22] G.N. Murshudov, A.A. Vagin, E.J. Dodson, Refinement of macromolecular structures by the maximum-likelihood method, *Acta Crystallogr. D: Biol. Crystallogr.* 53 (1997) 240–255.
- [23] D.E. McRee, XtalView/Xfit – a versatile program for manipulating atomic coordinates and electron density, *J. Struct. Biol.* 125 (1999) 156–165.
- [24] V.S. Lamzin, K.S. Wilson, Automated refinement of protein models, *Acta Crystallogr. D: Biol. Crystallogr.* 49 (1993) 129–147.
- [25] R.A. Laskowski, M.W. MacArthur, D.S. Moss, et al., PROCHECK: a program to check the stereochemical quality of protein structures, *J. Appl. Crystallogr.* 26 (1993) 283–291.
- [26] M.F. Sanner, Python: a programming language for software integration and development, *J. Mol. Graph. Model.* 17 (1999) 57–61.
- [27] M. Ingr, T. Uhlikova, K. Strisovsky, et al., Kinetics of the dimerization of retroviral proteases: the firemans's grip and dimerization, *Protein Sci.* 12 (2003) 2173–2182.